Harrison, P., Schubert, G., and Guo, Z. (2013) The behaviour of magneto-rheological elastomers under equi-biaxial tension. In: 19th International Conference on Composite Materials, 28 Jul - 2 Aug 2013, Montreal, Canada.

http://eprints.gla.ac.uk/85550/

Deposited on: 23 Jan 2014

THE BEHAVIOUR OF MAGNETO-RHEOLOGICAL ELASTOMERS UNDER EQUI-BIAXIAL TENSION

G. Schubert[1], P. Harrison[1*], Z. Guo[2]
[1] School of Engineering, University of Glasgow, Glasgow, UK
[2] Department of Engineering Mechanics, Chongqing University, Chongqing, China
* Corresponding author (Philip.harrison@glasgow.ac.uk)

Keywords: *Magneto-Rheological Elastomers, Smart Materials, Equi-biaxial Testing, Magnetic Fields*

1 Introduction

Equi-biaxial tension tests have been performed on isotropic and anisotropic magneto-rheological elastomers (MREs), a smart material whose mechanical properties can be instantaneously changed by applying a magnetic field.

MREs are a novel material with promising properties. The material has been tested in the small strain regime under various deformation modes [1-5] and there are a few applications developed employing MREs [1,3,6-8]. But there is still a lack of knowledge about large deformation performance of these smart materials. Uniaxial compression, tension and simple shear tests have been performed up to considerable large deformations [5,9-12], but a combination of different deformation modes is required to develop constitutive models. Biaxial tests on MREs have not yet been performed but are essential for developing and evaluating constitutive models.

A bespoke test rig was designed to facilitate testing of MREs under equi-biaxial deformations using a standard universal test machine. Samples were stretched to deformations of up to *10%* strain. A digital image correlation (DIC) system was used to measure strains. A magnetic field of *66.5mT* was applied to examine the change in stiffness of the specimens. The magneto-rheological (MR) effect is determined by calculating the tangent modulus as a function of engineering strain.

2 Experiments

2.1 Manufacturing of MREs

The MREs were manufactured using a silicone rubber (MM240TV from ACC Silicones) mixed with 30% silicone fluid (ACC34 from ACC Silicones) to reduce viscosity and stiffness of the final rubber. Carbonyl Iron Powder (CIP-SQ from BASF) with an average particle diameter of 4μm was used as the magnetic particulate phase of the composite. The volume fraction of the particles was varied from *0 to 30%*. All MREs were cured for *1.5* hours at *100°C*. Anisotropic samples were cured inside a magnetic field of *400mT* to achieve alignment of particles. The MRE samples were square sheets with a length of *50mm* and a thickness of *2mm*.

2.2 Test setup and procedure

A special test rig, designed in accordance with the British Standard [13], was manufactured to perform equi-biaxial tension tests using a universal test machine (Zwick Z250). The rubber sheets were held by three clamps on each side of the specimen; the clamps were free to slide along the frame as the test proceeded. To reduce friction and avoid any magnetisation, the rig and the sliding clamps were made of Teflon. The clamps for holding the rubber were made of aluminium and brass screws. An image of the test setup with permanent magnets parallel to the particle alignment for anisotropic samples is shown in Figure 1.

MREs undergo the stress softening behaviour known as the Mullins effect; an effect that is typical for all rubber materials [14,15]. As such, 4-cycles were used to precondition the specimens. Mean values and standard deviations of the third loading cycle were used to compare and interpret results. All tests were displacement controlled. The machine crosshead moved a total displacement of *10mm* upwards at a rate of *10mm/min* and the force in the vertical direction was recorded.

A digital image correlation system (3D-DIC System Limess) was used to determine strain. A random white speckle pattern was sprayed onto the samples and a series of images was taken during the test in order to calculate strains.
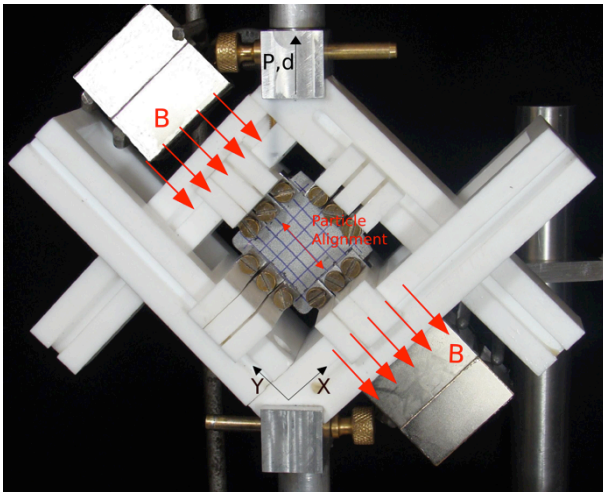
Fig 1: Test rig for equi-biaxial tension tests, permanent magnets and particle alignment of anisotropic MRE samples in y-direction.

The magnetic field was produced with strong permanent magnets (N52 Neodymium Magnets); two magnets were placed on each side of the test rig in order to create a magnetic field orientated parallel and perpendicular to the particle alignment (see Figure 1). Because of the large distance between the magnets a magnetic strength of only *66.5mT* was possible.

3 Experimental Results

3.1 Load-Displacement

Load and displacement in the vertical direction recorded by the universal test machine from the third loading cycle, both with and without the magnetic field, are shown in Figures 2 and 3.

The increase in stiffness when applying a magnetic field can be clearly seen (dashed lines in Figure 2). For anisotropic MREs, the magnetic field has been applied in two directions; both parallel and perpendicular to the particle alignment. Both magnetic field tests lead to very similar results (dashed and dotted lines in Figure 3). The MR effect appears to be at its highest for the isotropic and anisotropic MREs filled with 20% iron volume fraction.
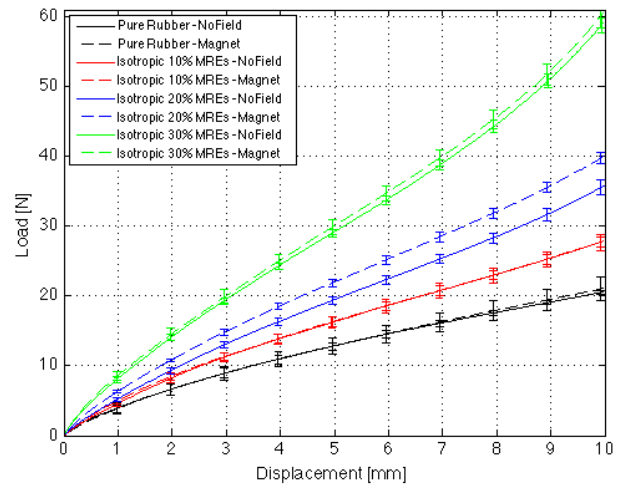
Fig 2: Load-Displacement curves of Pure Rubber and Isotropic MREs with *10, 20* and *30%* iron volume fraction. Tests without (solid line) and with magnetic field applied in the x-direction (dashed line).
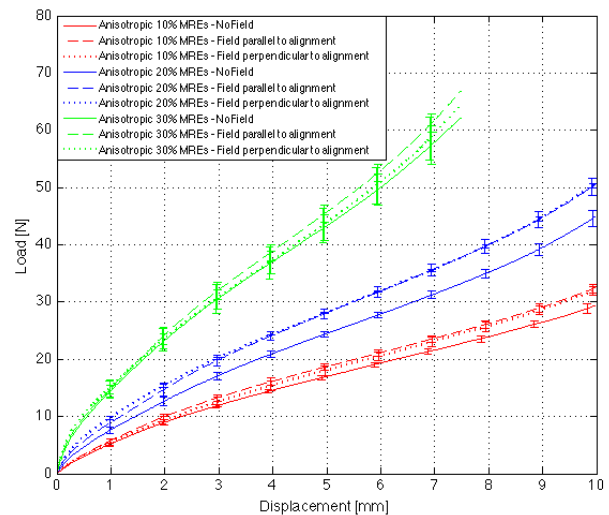

Fig 3: Load-Displacement curves of anisotropic MREs with *10, 20* and *30%* iron volume fraction. Tests without (solid line) and with the magnetic field, applied in both the y-direction (dashed line) and the x-direction (dotted line).

3.2 Digital Image Correlation (DIC)

A DIC system has been used to measure the strain distribution throughout the sample. Samples were sprayed with a white-paint speckle pattern and a series of images was recorded. *VIC-3D* software was used to perform correlation analysis. The software compares each image pattern in order to calculate displacements and the resulting strains. To double check results a grid was also drawn onto the samples

to enable manual calculation of strains by pixel measurement. These manual strain measurements were found to be in good agreement with the DIC results. The strain field along the x-direction of a pure rubber sample is shown in Figure 4.
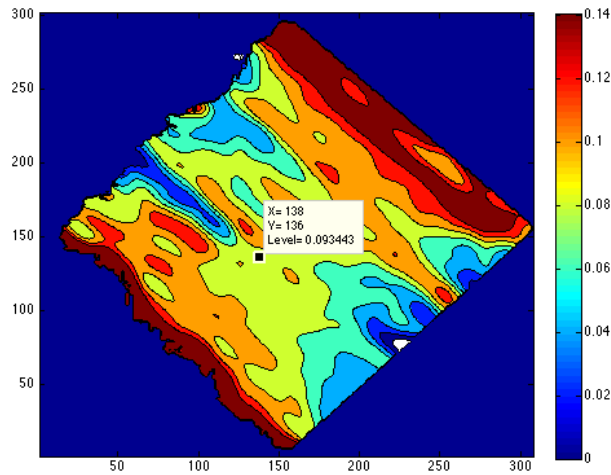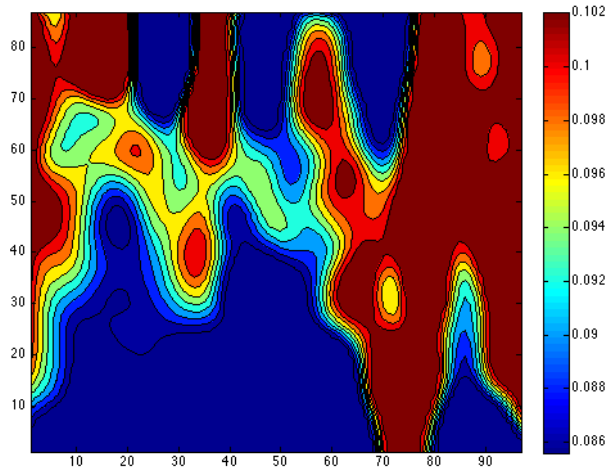

Fig 4: Engineering Strain of Pure Rubber under equi-biaxial tension, maximum strain in x-direction of the 3rd upload part, obtained from the DIC System Limess.

The strain field data shown in Figure 4 had to be processed. At first, the strain matrix was rotated for easier handling. A confidence interval provided by the DIC system was used to filter out unreliable strain values. Borders of the DIC strain field were cut, as strains close to the edges of the sample were either too high or too low due to the clamping of the MRE samples; *70%* of the strain field area was kept. The remaining strain field is shown in Figure 5.

As seen in Figure 5 the strain field within the selected area is nearly uniform with strain values ranging from about 8.6 to 10.2%. An average strain value for the DIC-produced strain field in this area was calculated and plotted against the time when the images were taken. This procedure was used for strains in both the x and y directions. Results of the 4-cycle test are plotted in Figure 6.

Linear fits to the strain versus time data (fitted separately to the loading and unloading cycles) shown in Figure 6, are used to convert displacement, provided by the test machine, to strain values provided by the DIC system. As expected, strain values in both directions are nearly identical. This was also found to be the case for both the anisotropic MRE samples and when applying the

magnetic field. The identical strain in both directions implies that the biaxial test rig is stiff enough to make a rigid body assumption when analysing the data.


Fig 5: Engineering Strain of Pure Rubber under equi-biaxial tension, maximum strain in x-direction of the 3rd upload cycle, the strain matrix was rotated, unreliable values eliminated and borders cut
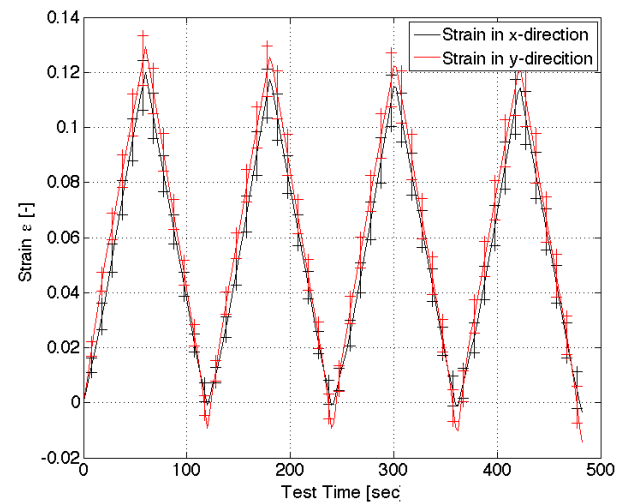
Fig 6: Engineering Strain of Pure Rubber in both stretching directions versus time, the complete 4-cycle test is illustrated.

3.3 Stress Calculation

The rigid body biaxial frame moves *10mm* upwards in the vertical direction. This movement imposes a strain and therefore a stress within the MRE samples. A linearly distributed force across the length, *w*, is assumed in order to simplify the analysis, as shown in Figure 7.
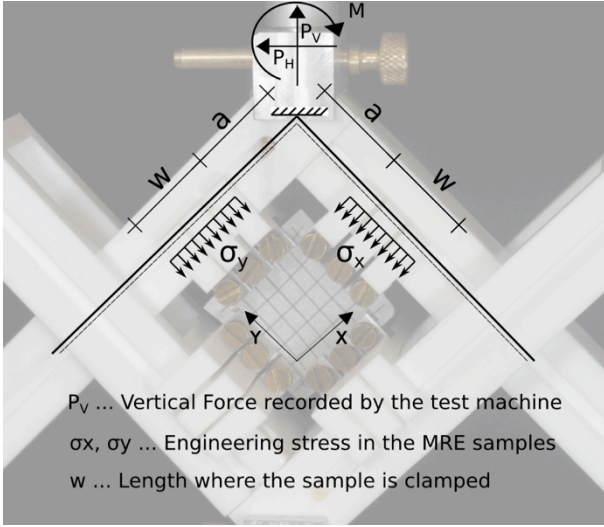
Fig 7: Structural system used to calculate the stresses in the stretching directions. The test rig is assumed to be a rigid body moving upwards causing a strain and stress within the MRE samples. Frictionless clamps are assumed.

The sliding clamps are assumed to be frictionless; forces along the frame axes are zero. Equilibrium is used to find the equation for the force, P, measured by the load cell of the test machine and for the stresses in both stretching directions, σ_x and σ_y. The structural system is illustrated in Figure 7. To calculate the stresses for an isotropic MRE sample where no magnetic field is applied is fairly straight forward. Analysis becomes more difficult for the case of the anisotropic samples and when a magnetic field is applied. Various assumptions are made in order to conduct the analyses, the validity of these assumptions is examined in Section 3.4. Five different cases can be distinguished:

I   Isotropic MREs tested without a magnetic field

The properties are the same for both the x and y directions. The stresses within the MRE sample can be calculated with

$$\sigma_x = \sigma_y = \frac{P_V}{\sqrt{2} \cdot t \cdot w} \tag{1}$$

where t is the thickness and w the width of the sample. The vertical force recorded by the test machine is P_v.

## II   Isotropic MREs tested with magnetic field applied in the x-direction

The magnetic field is assumed to change the properties of the MRE sample only in the x-direction. The stress in y-direction is assumed to remain the same as in Case I and is calculated using the mean value of the vertical force P_v recorded from the isotropic MRE samples when tested without a magnetic field, defined as $P_{Iso,NoField}$.

$$\sigma_y = \frac{P_{Iso,NoField}}{\sqrt{2} \cdot t \cdot w} \tag{2}$$

$$\sigma_x = \frac{\left[P_V - \frac{P_{Iso,NoField}}{2} \right] \cdot \sqrt{2}}{t \cdot w} \tag{3}$$

III   Anisotropic MREs with particle alignment in y-direction tested without magnetic field

In this case, in order to determine σ_y and σ_x, assumptions have to be made. From previously reported uniaxial tension tests [16], the anisotropic MRE samples are known to be stiffer in the direction of particle alignment, $\sigma_y \gg \sigma_x$. Stress versus displacement curves of the uniaxial tension tests are shown in Figure 8. In this and in all subsequent figures, the full length of the error bars indicates twice the standard deviation of the repeat results.
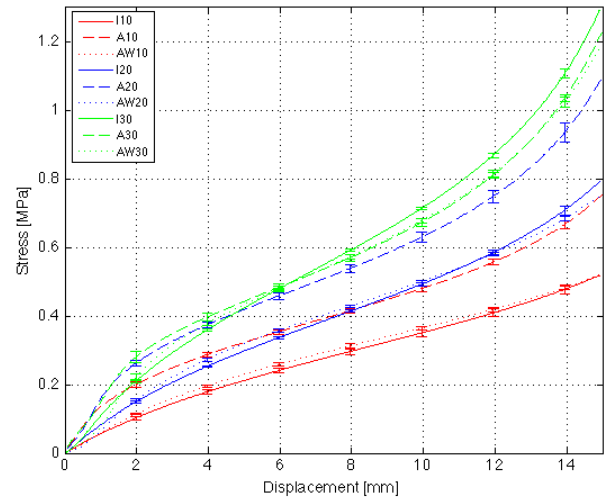
Fig 8: Stress-Displacement curves of uniaxial tension tests, Isotropic (I) and Anisotropic MREs with particle alignment along (A) and perpendicular to (AW) loading direction.
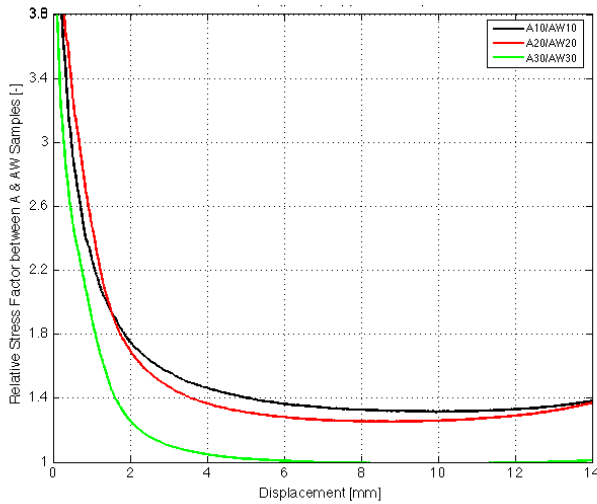
The relative stress factor between stresses of anisotropic samples with alignment in the loading direction, σ_A, and perpendicular to the loading direction, σ_{AW}, is used to evaluate the relationship between σ_x and σ_y in the biaxial tension tests.

$$f(d) = \frac{\sigma_A(d)}{\sigma_{AW}(d)} = \frac{\sigma_y}{\sigma_x} \qquad (4)$$

Mean values from three repeated tests are taken to calculate the relative stress factor, plotted versus displacement in Figure 9. The equilibrium condition is used to calculate stress in both stretching directions

$$\sigma_x = \frac{\sqrt{2}\cdot P_V}{t\cdot w\cdot(f(d)+1)} \qquad (5)$$

$$\sigma_y = \frac{\sqrt{2}\cdot P_V\cdot f(d)}{t\cdot w\cdot(f(d)+1)} \qquad (6)$$

Fig 9: Relative stress factor *f(d)* between anisotropic MREs with alignment in (A) and perpendicular to (AW) the loading direction tested in uniaxial tension. Note that the stress factor tends to infinity for small strain. Values below 2% strain are unreliable.

This method of using the relative stress factor, obtained from uniaxial tension tests, provides a means to perform a first approximate analysis of the biaxial test data. Constitutive models in combination with finite element analysis will be used to improve the analysis in future.

IV   Anisotropic MREs with particle alignment in y-direction, tested with the magnetic field also in the y-direction

The magnetic field is assumed to change the properties of the MRE sample, only in the y-direction. The stress in x-direction is assumed to stay the same as in Case III and is calculated with the mean value from three repeated tests. The vertical force P_v is taken from the anisotropic MRE samples tested without the magnetic field, defined as $P_{Aniso,NoField}$.

$$\sigma_x = \frac{\sqrt{2}\cdot P_{Aniso,NoField}}{t\cdot w\cdot(f(d)+1)} \qquad (7)$$

$$\sigma_y = \frac{\sqrt{2}}{t\cdot w}\left[P_V - \frac{P_{Aniso,NoField}}{f(d)+1}\right] \qquad (8)$$

V   Anisotropic MREs with particle alignment in y-direction tested with magnetic field in x-direction

The properties of the MRE sample are assumed to change only in the x-direction. The stress in y-direction is assumed to stay the same as in Case III, and is calculated using the mean value of the vertical force $P_{Aniso,NoField}$, defined and used already in Case IV.

$$\sigma_y = \frac{\sqrt{2}\cdot P_{Aniso,NoField}\cdot f(d)}{t\cdot w\cdot(f(d)+1)} \qquad (9)$$

$$\sigma_x = \frac{\sqrt{2}}{t\cdot w}\left[P_V - \frac{P_{Aniso,NoField}\cdot f(d)}{f(d)+1}\right] \qquad (10)$$

3.4 Validation of assumptions

To calculate MR effects the magnetic field is assumed to change properties of the MRE material only in the direction of action. To discuss the validity of this assumption, numerical predictions within the region occupied by the MRE sample were made. The multi-physics finite element software *COMSOL*[TM] *AC/*DC was used. The three-dimensional model of the two permanent magnets placed on either side of the sample, at a separation distance of *140mm* is illustrated in Figure 10.
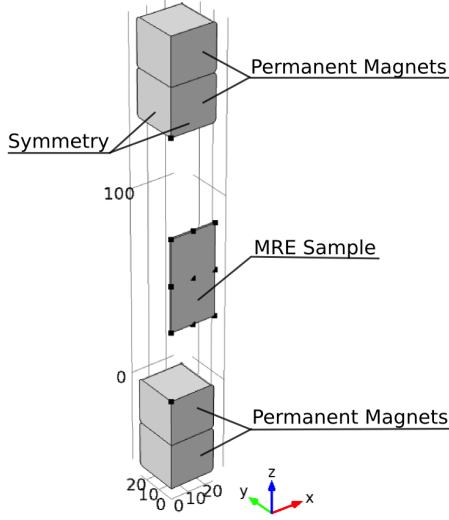
Fig 10: Three-dimensional model in *COMSOL*^{TM}, symmetry conditions are applied

The model is validated with experimental measurements of the magnetic induction at various positions using a Gaussmeter (Bell 5180). The magnetic flux density B_Z (along direction of action) and B_X (perpendicular to direction of action) is calculated for isotropic permeabilities ranging from $\mu=1$ to $\mu=5$. Earlier magnetic field measurements resulted in a permeability value of $\mu = 3.8$ for an isotropic MRE with *30%* volume particle concentration [17], which means the permeabilities considered here are within the range of those determined for real MRE material. Contour plots of the magnetic strength within the area of the MRE sample are plotted in Figure 11 ($\mu = 1$) and 12 ($\mu = 5$).
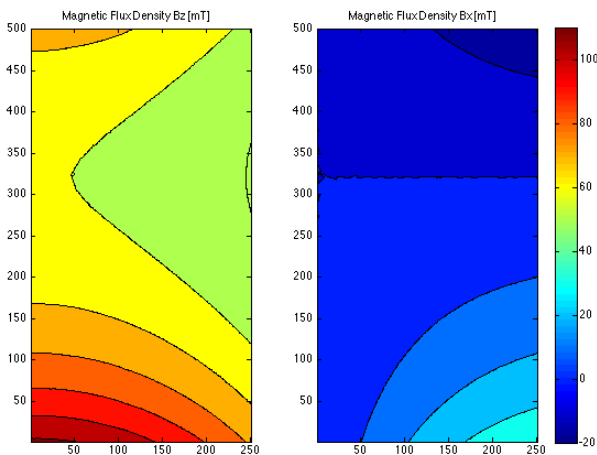
Fig 11: Magnetic Flux Density B [mT] within the area of the MRE sample, isotropic permeability $\mu = 1$, left) B_Z – Average value $B_{Z,mean} = 66.5\ mT$, right) B_x – Average value $B_{X,mean} = 4.1mT$
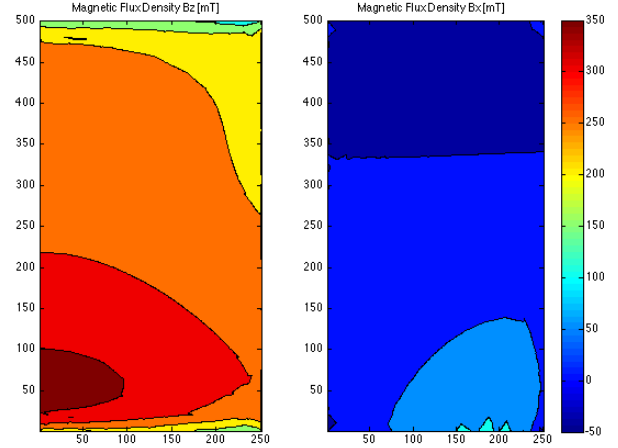
Fig 12: Magnetic Flux Density B [mT] within the area of the MRE sample, isotropic permeability $\mu = 5$, left) B_Z – Average value $B_{Z,mean} = 280.6\ mT$, right) B_x – Average value $B_{X,mean} = 16.1mT$

The magnetic flux in the x-direction is small compared to that in the z-direction. Factors between the average values of B_Z and B_X are calculated for each isotropic permeability and are listed in Table 1.

	$\mu = 1$	$\mu = 2$	$\mu = 3$	$\mu = 4$	$\mu = 5$
B_Z [mT]	66.5	126.1	181.2	232.5	280.6
B_X [mT]	4.2	7.7	10.8	13.6	16.1
B_Z / B_X	16.0	16.4	16.8	17.1	17.5

Table 1: Average Magnetic Flux Density B_Z and B_X *[mT]* within the area of the MRE sample and factor B_Z/B_X for isotropic permeability $\mu = 1$ to $\mu = 5$

For isotropic MRE samples the magnetic flux density in x-direction is less than *1/16* of the flux density in z-direction regardless of permeability. The magnetic field and therefore the MR effect in the x-direction is considered to be small enough to be neglected, validating the original assumption, at least for isotropic samples.

The analysis is more complicated in the case of anisotropic MRE samples. Also the permeability of those samples has to be considered as anisotropic which could lead to higher magnetic induction in x-direction for samples with particle alignment perpendicular to the magnetic field direction. Predictions in COMSOL^{TM} were made to calculate the factor B_Z / B_X (mean values are used) for different permeabilities, μ_x, in the horizontal direction and μ_z in vertical direction; results are illustrated in Figure 13.
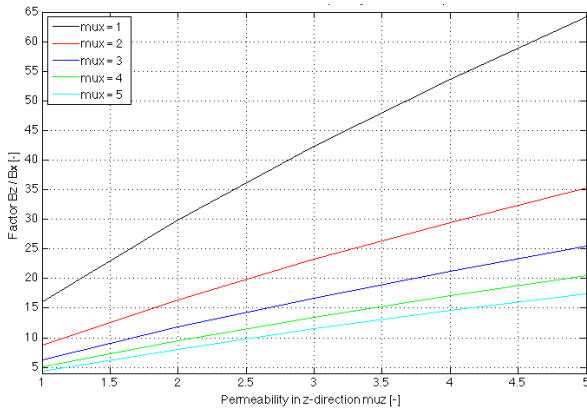
Fig 13: The volume averaged factor B_Z / B_X *[-]* in the specimen versus the magnetic permeability in the *z*-direction (co-incident with applied induction field) for different values of permeability in the *x* direction (perpendicular to the applied induction field). Values of the latter are provided in the figure legend.

The magnetic flux density in the horizontal direction is even smaller for MRE material with particle alignment in the magnetic field direction ($\mu_z > \mu_x$). However the factor B_Z / B_X approaches just 1 as the ratio $\mu_x / \mu_z = 5$ (see Figure 13). Given that magnetic field measurements from [17] suggested $\mu_x = 4.5$ and $\mu_z = 1$ for MRE samples with 30% volume particle content with particles aligned perpendicular to the magnetic field, it can be concluded that the magnetic field assumption is a poor approximation for such cases. In future, magnetic field predictions will be used to calculate the MR effects more accurately.

To calculate stresses for anisotropic MRE samples, the stress factor *f(d)* obtained from earlier uniaxial tension tests [16] is used. The procedure was described in Section 3.3 Case III. As seen in Figure 9 the stress factor tends to infinity for small strain values as the stresses are zero for zero strain. It should therefore be noted that the method of using a stress factor, *f(d)*, to interpret data can introduce significant errors for low strains and so small strain results, lower than 0.02 are considered to be less reliable than the data at higher strains.

3.5 MR Effect of Isotropic MREs

The procedures to calculate strains and stresses (Section 3.2 and 3.3) have been implemented in *MATLAB^TM*. Resulting stress-strain curves of isotropic MRE samples are shown in Figure 14 and 15. Mean values from at least three repeated tests on

different specimens using the third loading cycle have been used.
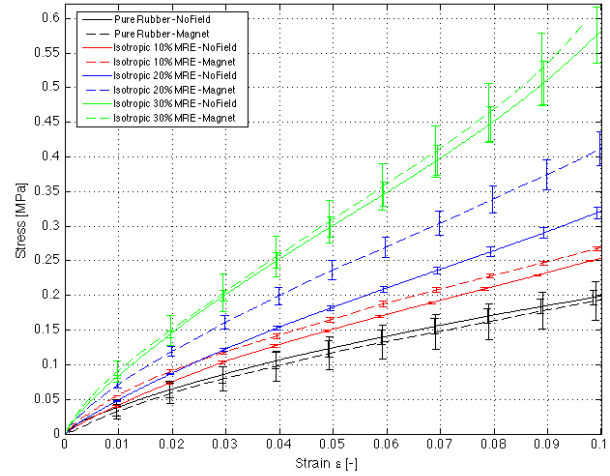
Fig 14: Stress versus strain in x-direction of Pure Rubber and Isotropic MREs with *10, 20* and *30%* of iron particles. Tests without (solid lines) and with a magnetic induction of *66.5mT* in x-direction (dashed lines) are compared
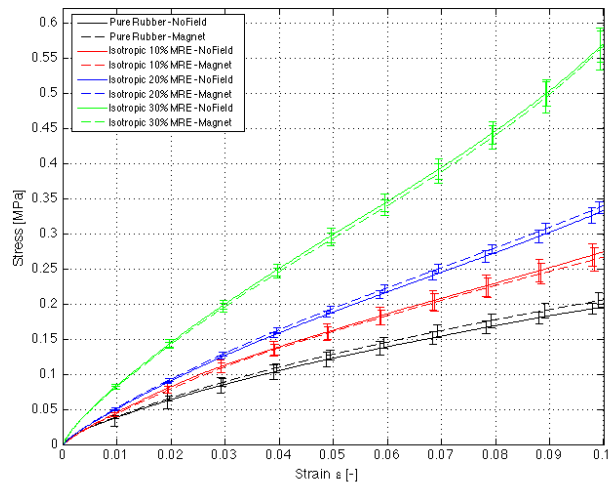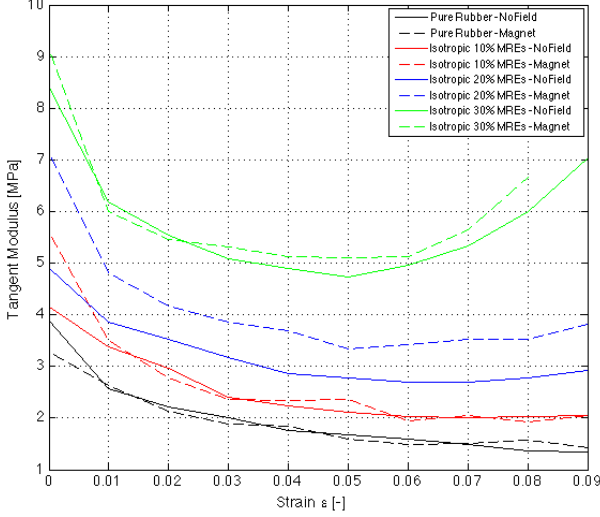

Fig 15: Stress versus strain in y-direction of Pure Rubber and Isotropic MREs with *10, 20* and *30%* of iron particles, Tests without (solid lines) and with a magnetic induction of *66.5mT* (dashed lines) are compared, stress in y-direction is not influenced by the magnetic field

In case of the isotropic MRE samples, a magnetic induction of *66.5mT* has been applied in the x-direction. As described in Case II (Section 3.3) the stress in y-direction is assumed to be the same for tests with and without magnetic field. The magnetic field is assumed to change the properties in the direction of the field only. As the material behaviour

is non-linear the tangent moduli are best plotted as a function of strain; *1%* strain increments are used to calculate the moduli. The results in the x-direction with and without magnetic field are illustrated in Figure 16.

Fig 16: Tangent Modulus versus strain in x-direction of Pure Rubber and Isotropic MREs with *10, 20* and *30%* of iron particles, Tests without (solid lines) and with a magnetic induction of *66.5mT* in x-direction (dashed lines) are compared, Tangent Moduli are calculated with 1% strain increments

Tangent moduli in y-direction are identical to those in the x-direction when tested without a magnetic field, as the material is isotropic (not illustrated here).

The relative MR effect is directly calculated from the tangent moduli and is defined with

$$MR_{rel} = \frac{E_M}{E_0} \qquad (11)$$

where MR_{rel} is the relative MR effect, E_M is the tangent moduli of tests with the magnetic field and E_0 is the moduli of tests without the magnetic field. The relative MR effect in both directions is plotted in Figure 17, where the effect in the y-direction is around one.

The Isotropic MREs with *20%* iron volume fraction shows the largest increase in moduli, by up to *45%* in the small strain region. The MR effect is still high, at about *1.25* at *9%* strain. This is a very good result considering the small magnetic induction of just *66.5mT*. Also, isotropic samples with *10%* iron

volume fraction demonstrate a reasonably high MR effect of *1.3* at small strains.
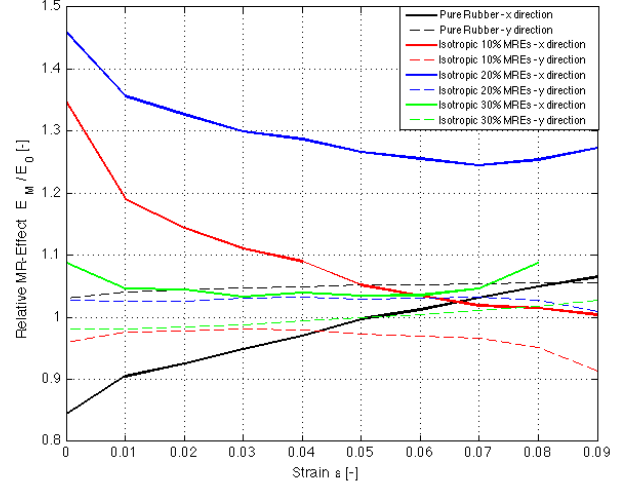
Fig 17: Relative Magneto-Rheological (MR) Effect versus strain of Pure Rubber and Isotropic MREs with *10, 20* and *30%* of iron particles, Magnetic field is applied in x-direction

Results on pure rubber indicate an experimental error of about *15%*. This error is possibly due to clamping issues due to for example, neglecting friction of the sliding clamps. Errors are also possible due to the DIC strain measurement technique. Isotropic MREs with *30%* iron particles show only an MR effect of 1.1. This is an unexpected result as MRE samples with 30% iron volume content tested under compression and tension did show high MR effects [16].

### 3.6 MR Effect for Anisotropic MREs

Analogous to Section 3.5, stresses, tangent moduli and MR effect versus engineering strain of anisotropic MRE samples are presented in this section. The stress values in the directions of stretch for anisotropic MREs are calculated using the relative stress factor determined using uniaxial tension tests, as described in Section 3.3 for Case III. Anisotropic samples have been tested with magnetic field parallel (y-direction) and perpendicular (x-direction) to the particle alignment direction. Stress-strain curves in the magnetic field direction are shown in Figure 18 and 19.

Note that the stress-strain curves of anisotropic samples in the *x*-direction (particle alignment perpendicular) have a low stress in the small strain region, up to *2%* strain (see Figure 19) while the stress-strain curves in *y*-direction (particle alignment

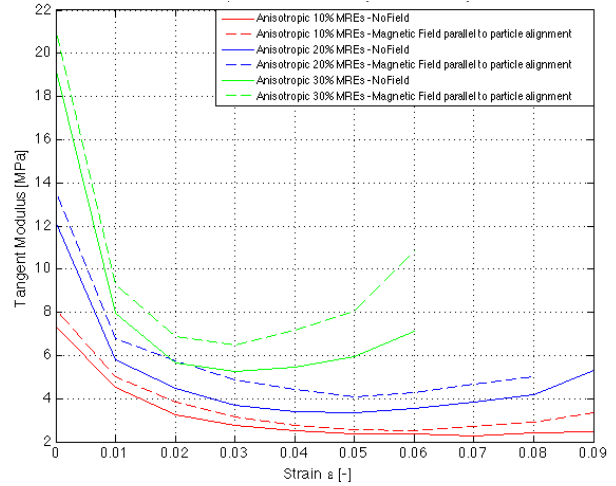parallel) start with a very steep slope (see Figure 18).
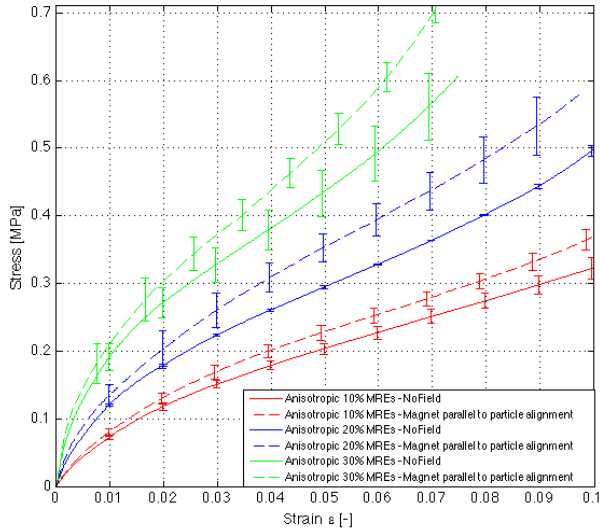
Fig 18: Stress versus strain in *y*-direction of anisotropic MREs with *10, 20* and *30%* of iron volume fraction. Tests both without (solid lines) and with a magnetic induction of *66.5mT* parallel to the particle alignment in y-direction (dashed lines) are compared.
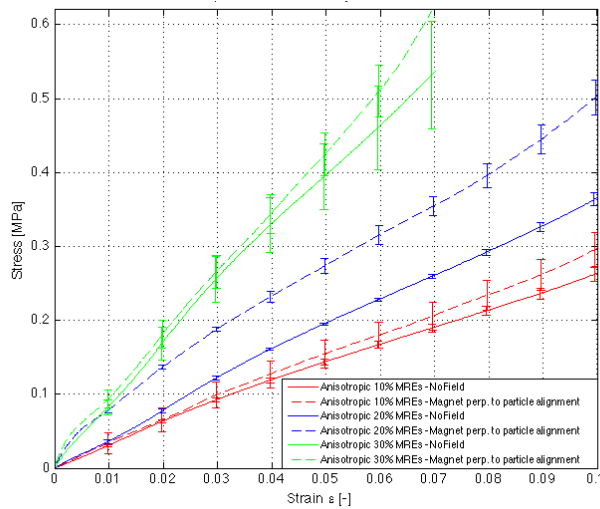
Fig 19: Stress versus strain in x-direction of anisotropic MREs with *10, 20* and *30%* of iron volume fraction. Tests both without (solid lines) and with a magnetic induction of *66.5mT* perpendicular to the particle alignment in *x*-direction (dashed lines) are compared.

The tangent moduli, calculated with *1%* strain increments, are illustrated in Figure 20 and 21. The tangent moduli in the *x*-direction for tests conducted without the magnetic field (see Figure 21) show very

low moduli in the small strain region. The moduli in the *x*-direction are possibly underestimated as a result of the analysis technique (due to the stress factor shown in Figure 9). The resulting relative MR effect could be overestimated.

Fig 20: Tangent modulus versus strain in y-direction for anisotropic MREs with *10, 20* and *30%* iron volume fraction. Tests both without (solid lines) and with a magnetic induction of *66.5mT* parallel to the particle alignment in y-direction (dashed lines) are compared.
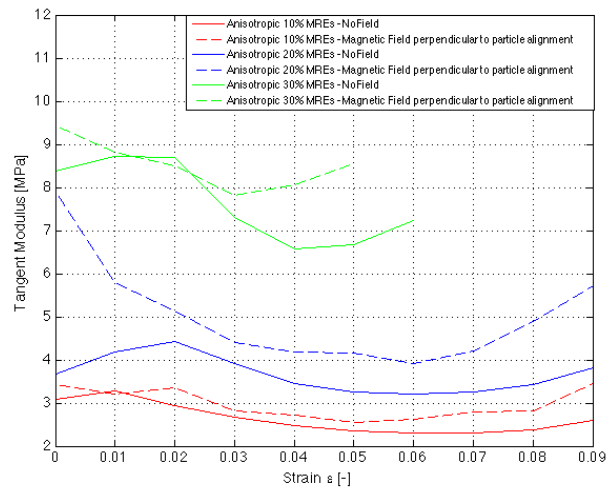

Fig 21: Tangent modulus versus strain in x-direction of anisotropic MREs with *10, 20* and *30%* iron volume fraction. Tests both without (solid lines) and with a magnetic induction of *66.5mT* perpendicular to the particle alignment in x-direction (dashed lines) are compared.

The relative MR effects calculated using equation 11, in the magnetic field direction are illustrated in Figure 22.
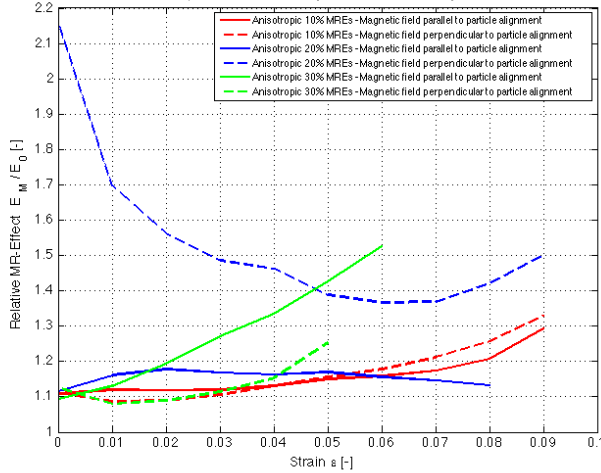
Fig 22: Relative Magneto-Rheological (MR) effect versus strain of anisotropic MREs with *10, 20* and *30%* iron volume fraction with the applied field parallel and perpendicular to the particle alignment

The anisotropic MREs with *20%* iron volume fraction and with the magnetic field applied perpendicular to the particle alignment show the highest relative increase. Note that values below *2%* strain are not considered to be very reliable. But still there is a 50% increase in moduli when applying a magnetic strength of 66.5mT, up to large strains of 9%. Varga found the 'most significant effect if the applied field is parallel to the particle alignment and to the mechanical stress' [11]. As discussed in section 3.4 the assumption that the magnetic field is only changing the properties of the material in the direction of action is a poor approximation in the case of perpendicular applied magnetic field. In future the MR effects will be calculated more accurately. All other MRE samples demonstrate a relative increase in moduli of about 10%. This is lower than the effects seen in the isotropic MREs when a field of *66.5mT* is applied.

4 Conclusions

Equi-biaxial tension tests have been performed on Magneto-Rheological Elastomers (MREs). A special test rig has been designed to enable testing on a universal test machine. Two permanent magnets on each side of the test rig created a magnetic flux

density of *66.5mT*. Tests on isotropic and anisotropic MREs with magnetic field parallel and perpendicular to the particle alignment direction were performed. A digital image correlation (DIC) system was used to evaluate strains. To calculate stresses in the two stretching directions, several assumptions were made:

1) Frictionless clamps; forces along the frame axes are zero.
2) The magnetic field changes the properties of the material only in the direction of the field.
3) In the case of anisotropic MRE samples it is assumed that the relation between stresses parallel and perpendicular to the particle alignment can be calculated with a relative stress factor taken from uniaxial tension tests.

The validity of assumption 2 and 3 is discussed in section 3.4. Tangent moduli are calculated from the stress-strain data using *1%* strain increments. Relative magneto-rheological (MR) effects are defined as a relative factor between tangent moduli of tests with and without magnetic induction; they are plotted versus engineering strain.

Isotropic MREs with *20%* iron volume fraction show a very high increase in moduli due to an MR effect of about *45%*. This steadily decreases down to about *25%* at larger strains of *9%*. The moduli of anisotropic MREs with the same content of iron increase about *50%* at large strains. Other MRE samples show lower MR effects. The moduli of isotropic samples with *10%* iron increase about *30%* in the small strain regime. Unexpectedly the samples with *30%* iron content show nearly no MR effect. The results of biaxial tension tests confirm the promising properties of MRE materials. MR effects are present in the small strain regime but also in larger strains.

To put these results into perspective, previous testing by the author on the same material under compression revealed a *60%* MR effect when high magnetic intensities of *400mT* were applied. Even higher MR effects of *400%* due to a magnetic induction of *280mT* were found when stretching MRE samples up to *50%* tensile strain. In both cases MR effects were highest in the small strain regime [16].Other researchers have found similar effects. Varga and Filipcsei [11] reached *75%* increase in moduli under compression when applying 400mT to an anisotropic MRE with particle alignment parallel

to the magnetic field. Farshad [10] achieved *140%* increase of the compressive modulus for isotropic MREs. Shen [18] tested MREs under simple shear up to *80%* strain and found *60%* increase in moduli when applying 400mT. Generally, the greatest MR effect was measured at low stains and tended to decrease with increasing strain.

Thus, considering the low magnetic induction of *66.5mT* applied during biaxial tension tests the achieved MR effects can be considered to be high.

This preliminary investigation into the use of this biaxial test was very informative and indicated the test could be a useful addition to the test methods currently used to characterise MREs. However, several improvements to the test can be suggested for future implementation. In particular using a torque load-cell in addition to the used uniaxial load-cell would make assumptions for stress distribution in anisotropic MRE samples and assumptions for the magnetic field unnecessary and improve the accuracy of the resulting data. A method of improving the clamping mechanism should be used to avoid unwanted boundary effects near the edge of the samples.

The experimental data of biaxial tests together with the uniaxial tests and the pure shear tests performed earlier will be used to develop constitutive models using the phenomenological approach in future.

References

[1] J. Ginder, W. Schlotter, M. Nichols, "Magnetorheo-logical Elastomers in Tunable Vibration Absorbers", *Smart Structures and Materials, Proceedings of SPIE,* Vol. 4331, pp 103-110, 2001

[2] M. Lokander, "Performance of Magnetorheological Rubber Materials", *Department of Fibre and Polymer Technology*, Royal Institute of Technology, PhD Thesis, Stockholm*,* 2004

[3] A. Albanese Lerner, "The Design and Implementation of a Magnetorheological Silicone Composite State-Switched Absorber", *School of Mechanical Engineering*, *Georgia Institute of Technology,* Master thesis*,* 2005

[4] J. Koo, F. Khan, D. Jang, H. Jung, „Dynamic characterization and modelling of magneto-rheological elastomers under compressive loadings *Smart Materials and Structures, Vol. 19,* 2010

[5] A. Boczkowska, S. Awietjan, S. Pietrzko, K. Kurzydlowskiowski, "Mechanical properties of magnetorheological elastomers under shear deformation", *Composites Part B: Engineering,* Vol. 43, pp 636-640, 2012

[6] L. Elie, J. Ginder, W. Stewart, M. Nichols, *"Variable stiffness bushing using magnetorheological elastomers"*, US Patent, 1997

[7] G. Hitchcock, F. Gordaninejad, A. Fuchs, *"Controllable magneto-rheological elastomer vibration isolator"*, US Patent, 2006

[8] R. Crist, *"Active vibrational damper"*, US Patent, 2009

[9] M. Kallio, "The elastic and damping properties of magnetorheological elastomers", *VTT Technical Research Centre of Finland, PhD Thesis,* 2005

[10] M. Farshad, M. Le Roux, "Compression properties of magnetostrictive polymer composite gels", *Polymer Testing*, Vol. 24, pp 163-168, 2005

[11] Z. Varga, G. Filipcsei, M. Zrinyi, "Magnetic field sensitive functional elastomers with tuneable elastic modulus", *Polymer,* Vol.47, pp 227-233, 2006

[12] G. Stepanov, A. Chertovich, E. Kramarenko, "Magnetorheological and deformation properties of magnetically controlled elastomers with hard magnetic filler", *Journal of Magnetism and Magnetic Materials, Vol. 324, pp 3448-3451,* 2012

[13] British Standard BS 903-5:2004 Physical Testing of Rubber, Part5: Guide to the application of rubber testing to finite element analysis

[14] L. Mullins, "Softening of Rubber by Deformation"*, Rubber Chemistry and Technology, Rubber Division, ACS*, Vol. 42, pp 339-362, 1969

[15] J. Diani, B. Fayolle, P. Gilormini, "A review on the Mullins effect", *European Polymer Journal, Vol. 45, pp 601 – 612, 2009*

[16] G. Schubert, P. Harrison, Z. Guo, "Characterisation of the magneto-rheological effect of silicone rubber – iron particle composites under large strain", 8th European Solid Mechanics Conference, Graz, 2012

[17] G. Schubert, P. Harrison, Z. Guo, "*The Magnetic Permeability of Isotropic and Anisotropic Magneto-Rheological Elastomers – Experimental Investigation and Simulations with Comsol"*, in preparation

[18] Y. Shen, M. Golnaraghi, G. Heppler, "Experimental Research and Modeling of Magnetorheological Elastomers", *Journal of Intelligent Material Systems and Structures,* Vol. 15, pp 27-35, 2004